

DOI: 10.1070/QEL16115

Investigation of lasing characteristics of domestic Yb:YAG laser ceramics

I.L. Snetkov, O.V. Palashov, V.V. Osipov, I.B. Mukhin,
R.N. Maksimov, V.A. Shitov, K.E. Luk'yashin

Abstract. **We report on the synthesis and laser characteristics of Yb^{3+}-doped yttrium aluminium garnet ($Y_3Al_5O_{12}$) optical ceramics. The ceramics was produced by solid-phase reactive sintering of a mixture of Yb (5 at %): Y_2O_3 and Al_2O_3 nanopowders synthesised by laser ablation, using additional calcination of the mixture before compaction. In a thin disk geometry, multiwatt laser oscillation was obtained at a wavelength of 1030 nm with a power of 5.2 W and a slope efficiency of 37.0 % at a pump pulse period-to-duration ratio of 5.72.**

Keywords: *nanopowder, optical ceramics, yttrium aluminium garnet, ytterbium, thin disk, lasing, slope efficiency.*

1. Introduction

Transparent polycrystalline materials based on yttrium aluminium garnet $Y_3Al_5O_{12}$ (YAG) doped with rare-earth ions (for example, Nd^{3+}, Yb^{3+}, Ho^{3+}) have drawn much attention since a group of Japanese scientists has succeeded in synthesising Nd:YAG ceramics with a high optical quality and in obtaining efficient lasing in this ceramics [1, 2]. Laser ceramics has the following advantages compared to single crystals: a lower synthesis temperature, the possibility of producing samples with large transverse sizes and a composite structure, and the possibility of forming a desired profile of dopant distribution in order to suppress parasitic thermal effects [3–5].

Owing to some properties, such as a high quantum efficiency, a broad gain band, and the absence of concentration quenching, active elements made of Yb:YAG ceramics are promising for application in solid-state lasers with high average and peak powers [6–8]. In recent years, several scientific groups obtained lasing in Yb:YAG ceramics synthesised using commercial powders of individual oxides [9, 10] or directly stoichiometric nanoparticles $Yb_{3x}Y_{3-3x}Al_5O_{12}$ [11, 12].

I.L. Snetkov, O.V. Palashov, I.B. Mukhin Institute of Applied Physics, Russian Academy of Sciences, ul. Ul'yanova 46, 603950 Nizhny Novgorod, Russia; e-mail: snetkov@appl.sci-nnov.ru, palashov@appl.sci-nnov.ru, mib_1982@mail.ru;
V.V. Osipov, V.A. Shitov, K.E. Luk'yashin Institute of Electrophysics, Ural Branch, Russian Academy of Sciences, ul. Amundsena 106, 620016 Ekaterinburg, Russia; e-mail: osipov@iep.uran.ru;
R.N. Maksimov Institute of Electrophysics, Ural Branch, Russian Academy of Sciences, ul. Amundsena 106, 620016 Ekaterinburg, Russia; Ural Federal University named after the First President of Russia B.N. Yeltsin, ul. Mira 19, 620002 Ekaterinburg, Russia; e-mail: romanmaksimov@el.ru

Received 20 April 2016
Kvantovaya Elektronika **46** (7) 586–588 (2016)
Translated by M.N. Basieva

However, the current literature provides no information about synthesis of Yb:YAG laser ceramics from nanopowders produced by laser ablation. Since the typical specific features of such nanoparticles (average size 10–15 mm, metastable crystal phase, high concentration of volatile components, and weak agglomeration) cause specific problems in the formation of nonporous structures, it is important to find techniques that can be used to synthesise ceramics of laser quality. The aim of this work is to synthesise the first domestic samples of Yb:YAG ceramics and to study their lasing characteristics.

2. Solid-phase synthesis of Yb:YAG laser ceramics

Nanoparticles Yb (5 at %): Y_2O_3 and Al_2O_3 needed to synthesise Yb:YAG ceramics were produced at the Institute of Electrophysics, Ural Branch, Russian Academy of Sciences (Ekaterinburg) by evaporation of a target material by the radiation of a repetitively pulsed CO_2 laser [13, 14]. To remove excessive volatile compounds and achieve the stoichiometric ratio (Yb + Y)/Al = 3/5, the obtained powders were transformed into the main cubic phase by calcination in air at temperatures of 900–1200 °C for 3 h. After weighting, the calcined powders were milled in a drum mill with an inclined rotational axis by yttria-stabilised zirconia (YSZ) balls in ethanol with addition of tetraethoxysilane (0.5 wt %) as a sintering additive.

To achieve partial phase transformation of particles into the Yb:YAG structure, the dried mixture of powders was additionally calcined in air at a temperature of 1200 °C for 3 h in order to equalise the rates of phase transformations and shrinkage, which ensures uniform compaction. Then, the mixture was milled once again and compacted by static uniaxial pressing with a pressure of 200 MPa. The Yb:YAG ceramics was synthesised in the process of sintering of the powder compact in a vacuum furnace with graphite heaters at a temperature of 1780 °C for 20 h. After sintering, the sample was annealed in air (1300 °C, 10 h) and polished to brilliance from both sides using diamond pastes.

3. Optical and lasing characteristics of Yb:YAG ceramics

The transmission spectrum of a 2-mm-thick Yb (5 at %):YAG ceramic sample measured on a Shimadzu UV-1700 spectrophotometer, as well as the theoretical transmission curve for YAG calculated by the known refractive index [15] is shown in Fig. 1. The transmission coefficient of the studied ceramic sample in the IR region reaches 81.8 %, which is 2 % lower

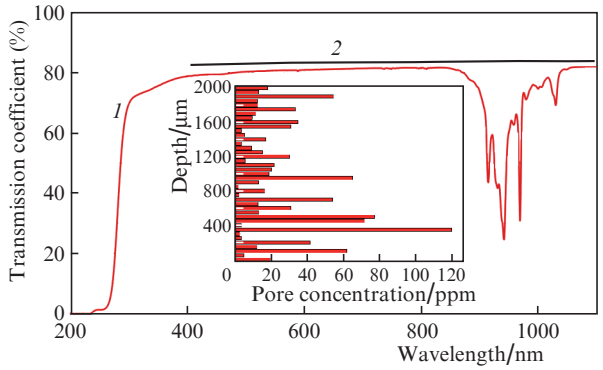

Figure 1. Transmission spectrum of a 2-mm-thick Yb:YAG ceramic sample (*1*) and theoretical transmission for YAG (*2*). The inset shows the distribution of pores over the ceramic sample depth.

than the calculated value. The absorption bands in the wavelength range 900–1400 nm are caused by the optical transitions in the ytterbium ion.

To determine the main microstructural defects that limit the material transparency, we studied the ceramics using an Olympus BX51TRF optical microscope. According to the obtained data, the structure of the sample consists of closely packed crystallites with an average diameter of 15 μm. In addition, there were observed spherical pores with diameters up to 6 μm, which are mainly localised at inter-crystallite boundaries. The average concentration of pores was determined by direct count to be 29 ppm (the inset in Fig. 1). The formation of pores can be caused by inhomogeneous compacting of the powder due to the existence of hard agglomerates formed in the process of calcination of nanoparticles in air. The presence of a residual porosity leads to the appearance of scattering of propagating radiation and, as a result, to an increase of losses in the ceramic element. The level of the scattered radiation for the studied sample was estimated according to works [16–18] to be 2.3% of the propagating radiation power, which corresponds to the scattering losses of 0.12 cm^{-1}.

To make an active element for a disk laser, the thickness of the Yb:YAG ceramic sample was decreased to 300 μm and the sample faces were coated with dielectric layers [an antireflection layer on one side and a mirror layer on the other side for the pump (940 nm) and laser (1030 nm) wavelengths]. For effective cooling, the active element with dielectric coatings was mounted on a water-cooled copper heat sink of the laser head using indium solder. The laser head was placed in a laser cavity. We used two types of laser cavities, namely, a linear cavity, which was formed by the rear face of the active element and dielectric input mirror (*6*) (Fig. 2a), and a V-shaped cavity formed by the rear face of the active element and two dielectric mirrors: spherical mirror (*7*) (with a radius of 30 mm and a reflectance $R \sim 100\%$ at a wavelength of 1030 nm) and output mirror (*6*) with reflectances of 90%, 95% and 98% at 1030 nm. The cavity arm was about 5 cm long.

Pumping was performed by a fibre-coupled diode laser (Laserline LDM 2000) emitting at a wavelength of 940 nm. Its radiation was focused by spherical mirror (*3*) on the studied sample into a spot 2 mm in diameter and, after one V-shaped pass through the sample, was deflected to an absorber; in this process, ~22% of radiation power was absorbed. For each of the cavity geometries, under quasi-cw pumping by pulses with a duration of 3.25 ms and a repetition rate of 148 ms, we

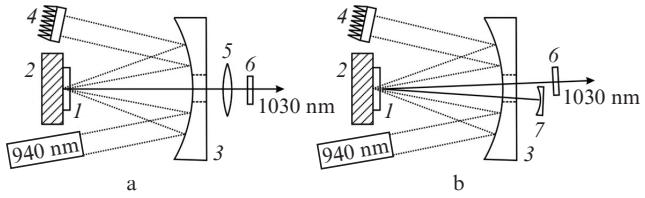

Figure 2. Schemes of the linear (a) and V-shaped (b) cavities of the thin-disk laser: (*1*) element under study; (*2*) heat sink of the laser head; (*3*) spherical mirror ($R \sim 100\%$ at $\lambda = 940$ nm); (*4*) absorber; (*5*) lens with dielectric antireflection coating at $\lambda = 1030$ nm; (*6*) plane output mirror; (*7*) spherical mirror ($R \sim 100\%$ at $\lambda = 1030$ nm).

observed free-running laser operation (Fig. 3a). The laser radiation power was recorded by Ophir 3A and Ophir 10A power meters. In the case of the linear cavity, the maximum slope efficiency ($\eta = 22.9\%$) was observed using the output mirror with the reflectance $R = 95\%$, while the maximum

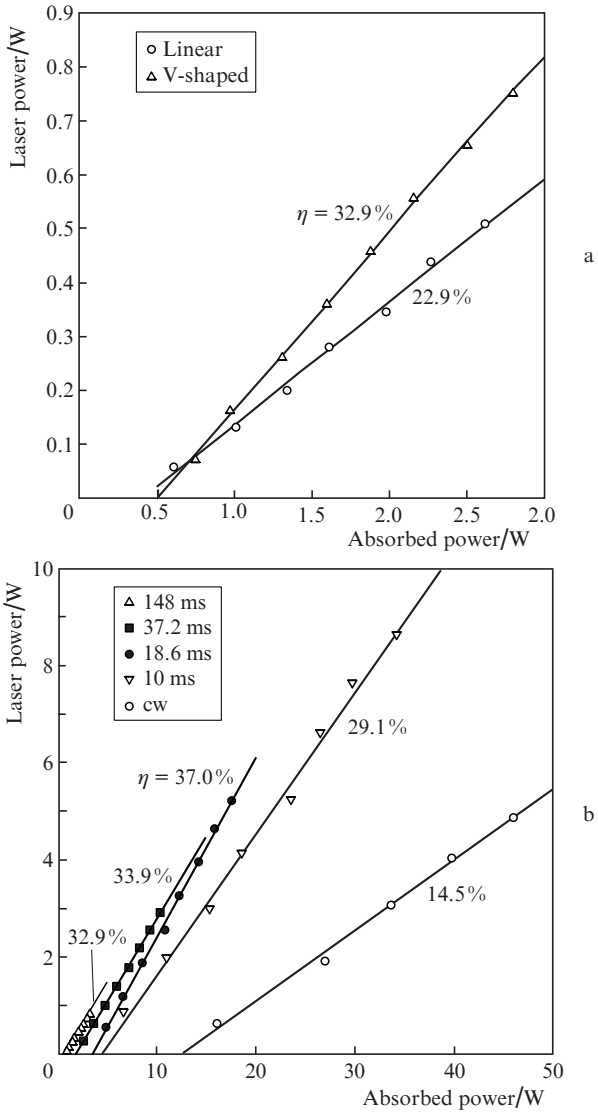

Figure 3. Dependences of the average output power on the average absorbed power in the case of linear and V-shaped laser cavities at a pump pulse repetition period of 148 nm (a), as well as in the case of the V-shaped cavity at different pulse repetition rates (b).

slope efficiency (η = 32.9%) in the case of the V-shaped pass was achieved using a mirror with the transmittance T = 90%. The difference in η can be explained by additional losses at the focusing lens used in the linear cavity. In the absence of lens (*5*), we failed to obtain laser oscillation.

In the case of the V-shaped cavity and a mirror with T = 90%, we measured the dependences of the output laser power on the absorbed pump power at different pump pulse repetition rates (Fig. 3b). The maximum slope efficiency η = 37% was observed at a repetition rate of 18.6 ms, which corresponds to a pulse-period-to-pulse-duration ratio of 5.72. With increasing pump pulse repetition rate, the slope efficiency decreased due to appearing thermal effects and reached 14.5% in the case of cw pumping. The occurrence of laser oscillation upon cw pumping points to a high quality of the ceramic material and to the possibility of its application for production of active elements. However, the ceramics quality is still lower than the quality of commercially available single crystals, which, under similar conditions, demonstrate lasing with an average power of hundreds of watts and an efficiency exceeding 40% [19, 20].

Thus, we have synthesised a sample of Yb (5 at %): $Y_3Al_5O_{12}$ ceramics from nanopowders produced by laser evaporation. We have studied its optical quality and demonstrated repetitively pulsed lasing with a slope efficiency of 37%. Under cw pumping by laser diodes, the slope efficiency was 14.5%.

Acknowledgements. The authors thank Prof. Ken-ichi Ueda for his contribution to the analysis of the results and for discussion of the paper.

The work on the ceramics synthesis was fulfilled in the frame of State Task Project No. 0389-2014-0027 (2016–2017) and supported by Act 211 of the Government of the Russian Federation (Contract No. 02.A03.21.0006). The study of laser properties was supported by the mega-grant of the Government of the Russian Federation (Grant No. 14. B25.31.0024), executed at Institute of Applied Physics.

References

1. Ikesue A., Furusato I., Kamata K. *J. Amer. Cer. Soc*., **78**, 225 (1995).
2. Ikesue A., Kinoshita T., Kamata K., Yoshida K. *J. Am. Ceram. Soc*., **78**, 1033 (1995).
3. Ikesue A., Aung Y.L. *Nat. Photon*., **2**, 721 (2008).
4. Liu W., Li J., Jiang B., et al. *J. Alloys Compd*., **538**, 258 (2012).
5. Osipov V.V., Shitov V.A., Solomonov V.I., Lukyashin K.E., Spirina A.V., Maksimov R.N. *Ceram. Int*., **41**, 13277 (2015).
6. Latham W.P., Lobad A., Newell T.C., Stalnaker D. *Proc. AIP Conf.*, **1278**, 758 (2010).
7. Banerjee S., Ertel K., Mason P.D., Phillips P.J., De Vido M., Smith J.M., Butcher T.J., Hernandez-Gomez C., Greenhalgh R.J.S., Collier J.L. *Opt. Express*, **23**, 19542 (2015).
8. Albach D., Chanteloup J.-C. *Opt. Express*, **23**, 570 (2015).
9. Wu Y., Li J., Pan Y., Guo J., Jiang B., Xu Y., Xu J. *J. Am. Ceram. Soc.*, **90**, 3334 (2007).
10. Luo D., Zhang J., Xu C., Qin X., Tang D., Ma J. *Opt. Mater*., **34**, 936 (2012).
11. Takaichi K., Yagi H., Lu J., Shirakawa A., Ueda K., Yanagitani T., Kaminskii A.A. *Phys. Stat. Sol. A*, **200**, R5 (2003).
12. Dong J., Shirakawa A., Ueda K., Yagi H., Yanagitani T., Kaminskii A.A. *Appl. Phys. Lett*., **89**, 091114 (2006).
13. Osipov V.V., Kotov Y.A., Ivanov M.G., Samatov O.M., Lisenkov V.V., Platonov V.V., Murzakaev A.M., Medvedev A.I., Azarkevich E.I. *Laser Phys*., **16**, 116 (2006).
14. Osipov V.V., Platonov V.V., Lisenkov V.V., Podkin A.V., Zakharova E.E. *Phys. Stat. Sol. C*, **10**, 926 (2013).
15. Kaminskii A.A., Ueda K., Konstantinova A.F., Yagi H., Yanagitani T., Butashin A.V., Orekhova V.P., Lu J., Takaichi K., Uematsu T., Musha M., Shirokava A. *Crystallogr. Rep*., **48**, 868 (2003).
16. Balabanov S.S., Bykov Y.V., Egorov S.V., Eremeev A.G., Gavrishchuk E.M., Khazanov E.A., Mukhin I.B., Palashov O.V., Permin D.A., Zelenogorsky V.V. *Opt. Mater*., **35**, 727 (2013).
17. Snetkov I.L., Mukhin I.B., Balabanov S.S., Permin D.A., Palashov O.V. *Kvantovaya Elektron*., **45**, 95 (2015) [*Quantum Electron*., **45**, 95 (2015)].
18. Snetkov I.L., Mukhin I.B., Palashov O.V. *Kvantovaya Elektron*., **46**, 193 (2016) [*Quantum Electron*., **46**, 193 (2016)].
19. Kuznetsov I.I., Mukhin I.B., Vadimova O.L., Palashov O.V. *Kvantovaya Elektron*., **45**, 207 (2015) [*Quantum Electron*., **45**, 207 (2015)].
20. Kuznetsov I.I., Mukhin I.B., Palashov O.V. *Laser Phys*., **26**, 045004 (2016).